Article ID: 1007-7294(2021)10-1356-11

Crack Evaluation of an Ultra-High-Pressure Chamber Used for Deep-Sea Environment Simulation

WU Mian[1], *WANG Fang*[2,3], *LUO Rui-long*[3], *JIANG Zhe*[3], *CUI Wei-cheng*[3,4]

(1. Jiangsu Provincial Key Laboratory of Advanced Manufacture and Process for Marine Mechanical Equipment, Jiangsu University of Science and Technology, Zhenjiang 212003, China; 2. Shanghai Engineering Research Center of Marine Renewable Energy, College of Engineering Science and Technology, Shanghai Ocean University, Shanghai 201306, China; 3. Shanghai Engineering Research Center of Hadal Science and Technology, College of Marine Sciences, Shanghai Ocean University, Shanghai 201306, China; 4. Westlake University, Hangzhou 310024, China)

Abstract: Ultra-high-pressure (UHP) thick chamber for simulating the underwater pressure environment bears high cyclic load and is prone to cracks caused by fatigue. Fatigue crack growth is an important factor affecting their fracture. The objective of this paper is to analyze the behavior of semi-elliptical crack growth in an aged UHP chamber and to estimate the safety margin of the chamber. For this purpose, crack growth properties of the material 20MnMoNb steel were experimentally investigated first considering triangular and trapezoidal load history respectively. Two series of results were compared to examine the sensitivity of the material on holding time. A three-dimensional finite element (FE) model was used for fatigue crack growth calculation based on the unified crack growth rate model and verified by comparing groups of numerical and experimental results on CT specimen. A series of FE models for cracks with different initial size, aspect ratio and inclination level are presented and residual life of the chamber is obtained based on the allowable criterion depth of surface cracks on the inner wall of the chamber. The analysis results will be used as a reference to evaluate the reliability of the UHP chamber.

Key words: ultra-high-pressure chamber; crack growth; pressure vessel; deep-sea environment simulation; residual life

CLC number: U663.8 **Document code:** A **doi:** 10.3969/j.issn.1007-7294.2021.10.008

0 Introduction

Deep sea exploration attracts human's attention in recent years, which has led to an upsurge in research and development of deep-sea equipment. Pressure tests on the structure strength and sealing performance are required for components of deep-sea equipment before they are applied in deep-sea to ensure safety. These pressure tests will be carried out in ultra-high-pressure (UHP) thick chambers for simulating the underwater pressure environment with its pressure-resistant

Received date: 2021-04-19

Foundation item: Supported by the National Natural Science Foundation of China (52071203); the General Program of Natural Science Foundation of Shanghai Committee of Science and Technology (19ZR1422700); the Project of Shanghai Engineering Research Center of Marine Renewable Energy (19DZ2254800)

Biography: WU Mian(1993-), male, master student;
WANG Fang(1979-), female, associate professor, E-mail: wangfang@shou.edu.cn.

(C)1994-2021 China Academic Journal Electronic Publishing House. All rights reserved. http://www.cnki.net

structure, as shown in Fig. 1 for illustration of a component pressured in the UHP chamber.

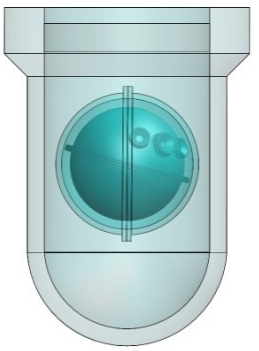

Fig.1 Sketch of UHP chamber for deep-sea environment simulation

Research has been done on the design and analysis of a variety of UHP chamber systems with the functions of pressure resistance, water-tightness, detecting leaks, video transmission etc.[1-5]. The core problem of pressured hull design is to examine the ability of the hull to resist deformation and damage under the action of load[6-8], that is, to guarantee its strength, stiffness and stability, and to ensure the safety. UHP chambers used for deep-sea environment simulation with the form of a typical cylindrical shell are of normal temperature chambers. And the design internal medium pressure may be higher than hundred mega-pascals and much greater than the external pressure. The failure form of a general internal pressure hull such as underwater pipelines includes leakage, rupture and excessive deformation or even destruction[9-10]. Strength failure criteria with fatigue and fracture failure included will be adopted to avoid leakage or structural loss stability.

However, micro-cracks as shown in Fig. 2 are sometimes buried below the surface of shell which can expand under severe stress. Strict flaw detection should be performed before use. Undetected defects may grow to new macro-cracks especially near the surface due to the interaction of more rigorous stress processes, which may propagate along the wall thickness direction. Fatigue crack growth properties must be taken into account.

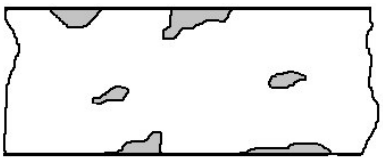

Fig.2 Sketch of the distributed micro-cracks inside the material

Most of studies on crack growth in pressure vessels are carried out in pipe and nuclear industries. Margolin and Karzov[11] applied the fatigue crack propagation model based on the analysis of material behavior in the local zones near the crack tip on nuclear pressure vessels made of 2CrMoNiV. Price and Ibrahim[12] studied crack growth in aluminum cylinders with cracks initiating at the neck shoulder of nuclear vessels. Meaningful results are obtained for damage tolerance analysis. Tan et al[13] presented creep constraint and fracture parameter for axial semi-elliptical surface cracks with high aspect ratio in pressurized pipes made of 25Cr2NiMo1V steel, in which creep life assessment method was provided. Various studies can be found in other literatures[14-17]. The researchers of these studies have grasped some methods and laws of crack propagation in pressure vessels from different levels, but they have not paid enough attention to ultra-high pressure thick-walled vessels.

The UHP chambers equipped in the authors' laboratory have been in use for more than five years. In order to ensure the safety of the pressure chambers, it is necessary to evaluate their performance in a comprehensive way. At present, it is difficult to detect the inner walls of the UHP chambers totally. However, according to past experience, there will inevitably be some severe deformation and surface defects in the inner walls after cycles of high pressure. These surface defects can be conservatively treated as surface cracks. The evaluation of the cyclic capacity of the cracked bodies can be specified. 20MnMoNb steel is a material which is usually used for construction of such

(C)1994-2021 China Academic Journal Electronic Publishing House. All rights reserved. http://www.cnki.net

chambers. But the crack growth data are not enough. In this paper, the crack growth properties of the material under two types of loading conditions are experimentally studied to examine the sensitivity of the material on holding time. Then a numerical study on a certain UHP chamber with semi-elliptical cracks in the internal side is established to evaluate its safety against fracture and fatigue failure under acceptable crack size criterion.

1 Problem description

1.1 Structure and material

The analyzed UHP chamber has an inner diameter of 450 mm and an outer diameter of 890 mm, which was designed for simulating the full ocean depth environment with a pressure of 115 MPa. Its configuration is shown in Fig.3. It is a cylindrical thick-walled structure with a flat cover.

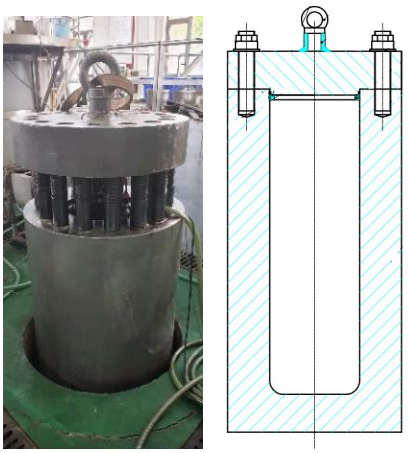

Fig.3 Configuration of UHP chamber

The chamber is made of 20MnMoNb steel. The chemical composition ratio of the material is listed in Tab.1. Four tensile samples tested to obtain the mechanical properties of the material are listed in Tab.2, showing a satisfactory plasticity and high strength.

Tab.1 Chemical composition of material 20MnMoNb steel (weight%)

C	Mn	Si	S	P	Cr	Ni	Mo	Cu	Nb
0.20	1.43	0.31	0.002	0.007	0.043	0.052	0.50	0.05	0.033

Tab.2 Material mechanical properties

Specimen No.	ε/%	Z/%	σ_y/MPa	σ_b/MPa	E/GPa
1#	24.76	73.17	586	687.9	210.8
2#	27.32	68.42	572	677.7	209.4
3#	27.48	69.53	566	672.5	210.7
4#	23.04	72.12	597	701.9	209.5
Average	25.65	70.81	580	685.0	210.1

Note: ε-elongation; Z-area reduction; σ_y-yield strength; σ_b-ultimate tensile strength; E-elastic modulus

1.2 Loading history

In the course of service, deep-sea equipment will bear the pressure of sea water, and the pressure will change with the process of dive-operation-float for many times, that is to say, it will bear the effect of cyclic load. Both the static strength and fatigue strength of the equipment need to meet the requirements. In the process of strength checking and fatigue checking of these components by means of a UHP chamber, the chamber itself is also affected by cyclic load. In addition, it is sometimes necessary to consider whether the retaining load during the operation in deep sea has an impact on the component. Fig.4 records the pressure of the chamber analyzed in the present study during a certain period of time. Retaining load exists in some loading cycles for several minutes or even

(C)1994-2021 China Academic Journal Electronic Publishing House. All rights reserved. http://www.cnki.net

hours. Generally, in fatigue analysis, the treatment of similar trapezoidal loads can be approximated by linear superposition method. Crack propagates under the joint action of triangular cyclic load and retaining load. The crack growth may be different under the two load sequences respectively, as shown in Fig.5(a) and Fig.5(b). But the extent of difference also depends on the properties of the material itself and the duration of magnitude of the sustaining load. Research on the dwell fatigue properties of several candidate high strength alloy materials used in deep sea equipment were conducted by Wang et al[18-19]. Dwell fatigue properties of the present material for UHP chambers 20MnMoNb steel have not been reported yet. Fatigue life analysis based on fracture mechanics needs considering the effect of sustaining load on crack growth performance of the material which is presented in the next section.

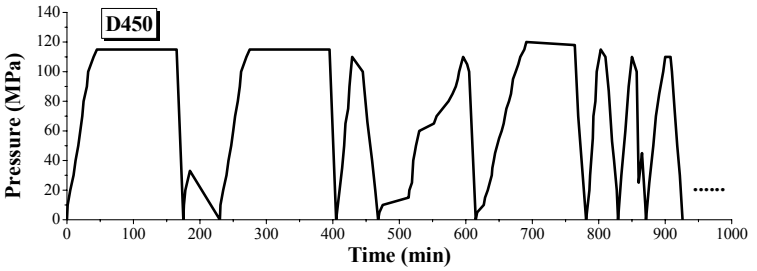

Fig.4 Loading history of the ultra-high-pressure chamber (with an inner diameter of 450 mm)

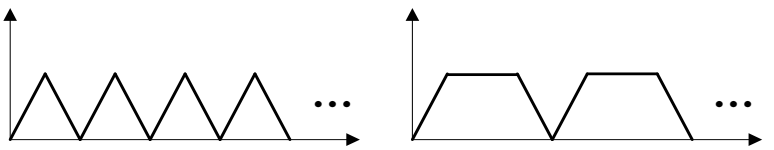

(a) Triangular load history (b) Trapezoidal load history

Fig.5 Sketch of two types of simplified loading histories

1.3 Crack growth properties by experiments

The crack propagation rate test was carried out on MTS810 fatigue testing machine. The standard compact tensile specimens (hereinafter referred to as CT specimens) with W=60 mm, B=15 mm and a_0=12 mm are used to prefabricate cracks of 1-2 mm. The test was carried out in room temperature, using sine wave loading mode with a loading frequency of 10 Hz and the maximum load is 20 kN with a stress ratio of 0. The time of holding load determines the cost of test. To save the test cost, the reference time of retaining load in the present study was set to 2 minutes.

The crack growth rate da/dN is obtained from the a-N curve. The magnitude of the stress intensity factor ΔK is calculated as follows:

$$\Delta K = f(a/W)\frac{\Delta F}{BW^{0.5}} \tag{1}$$

$$f(a/W) = \left(2 + \frac{a}{W}\right)\frac{0.886 + 4.64\left(\frac{a}{W}\right) - 13.32\left(\frac{a}{W}\right)^2 + 14.72\left(\frac{a}{W}\right)^3 - 5.6\left(\frac{a}{W}\right)^4}{\left(1 - \frac{a}{W}\right)^{1.5}} \tag{2}$$

where a is the crack length, W is the sample width, B is the sample thickness, and ΔF is the load magnitude.

(C)1994-2021 China Academic Journal Electronic Publishing House. All rights reserved. http://www.cnki.net

The experimental results of two a–N curves under normal fatigue loading (triangular load history) and dwell fatigue loading (trapezoidal load history) are shown in Fig. 6. The crack growth rate curves (da/dN~ΔK curves) are shown in Fig. 7. In the stable growth stage, the two curves almost coincide, and the crack growth is not affected by the sustaining load.

A unified crack growth rate model (UCGRM) proposed by Cui et al (2013) will be used for crack growth calculation, which can be expressed by the following equations,

$$\mathrm{d}a/\mathrm{d}N = \frac{A\left[\Delta K_{\mathrm{eff}} - \Delta K_{\mathrm{effth}}\right]^{m}}{1 - \left(K_{\max}/K_{\mathrm{Cf}}\right)^{n}} \tag{3}$$

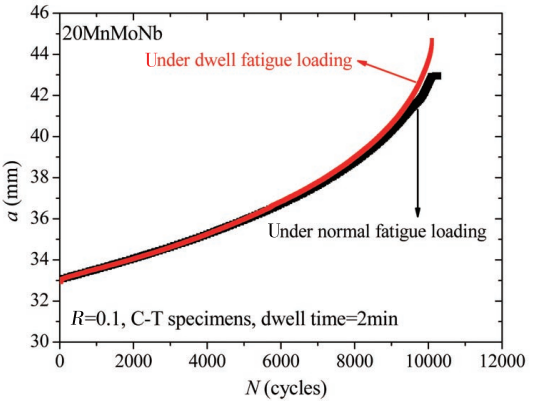

Fig.6 Crack length versus cycles (a–N curve) under dwell fatigue loading (triangular load history) and normal fatigue loading (trapezoidal load history)

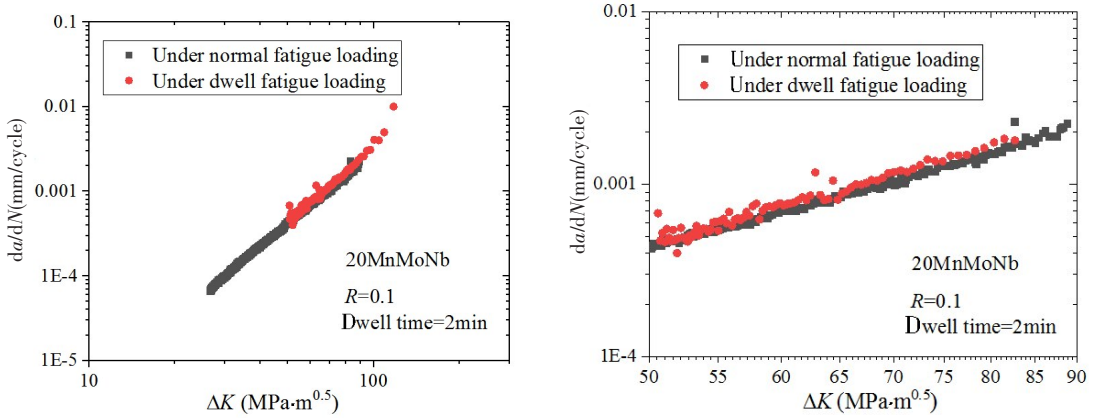

(a) Total test results (b) Test results in linear region

Fig.7 Crack growth rate curves (da/dN~ΔK curve) under normal fatigue loading (triangular load history) and dwell fatigue loading (trapezoidal load history)

where, $\Delta K_{\mathrm{eff}} = \begin{cases} K_{\max}\cdot\left(1 - f_{\mathrm{op}}\right), R < 0.7 \\ K_{\max} - K_{\min}, \quad R \geqslant 0.7 \end{cases}$ and $\begin{cases} K_{\max} = \sqrt{\pi r_{\mathrm{e}}\left(\mathrm{Sec}\dfrac{\pi}{2}\dfrac{\sigma_{\max}}{\sigma_{\mathrm{v}}} + 1\right)}\left(1 + Y(a)\sqrt{\dfrac{a}{2r_{\mathrm{e}}}}\right)\sigma_{\max} \\ \dfrac{\sigma_{\mathrm{v}}}{\sigma_{\mathrm{u}}} = \dfrac{\pi}{2}\cdot\dfrac{1}{\cos^{-1}\left(\dfrac{1}{\alpha^2 - 1}\right)}, \alpha = \dfrac{K_{\mathrm{IC}}}{\sigma_{\mathrm{u}}\sqrt{\pi r_{\mathrm{e}}\left(1 + \dfrac{Y\left(r_{\mathrm{e}}\right)}{\sqrt{2}}\right)}} > \sqrt{2} \end{cases}$

$$f_{\mathrm{op}} = \begin{cases} \max\left\{R, A_0 + A_1 R + A_2 R^2 + A_3 R^3\right\}, 0 \leqslant R < 1 \\ A_0 + A_1 R, \qquad\qquad -2 \leqslant R < 0 \end{cases}$$

$$\begin{cases} A_0 = \left(0.825 - 0.34\alpha' + 0.05\alpha'^2\right)\cdot\left[\cos\left(\pi\sigma_{\max}/2\sigma_{\mathrm{fl}}\right)\right]^{1/\alpha'}; A_1 = \left(0.415 - 0.071\alpha'\right)\cdot\sigma_{\max}/\sigma_{\mathrm{fl}} \\ A_2 = 1 - A_0 - A_1 - A_3; A_3 = 2A_0 + A_1 - 1; \sigma_{\mathrm{fl}} = \left(\sigma_{\mathrm{Y}} + \sigma_{\mathrm{u}}\right)/2 \\ \alpha' = 1/(1 - 2\nu) + \left[1 - 1/(1 - 2\nu)\right]/\left[1 + 0.886\,1\cdot\left(t/\left(K_{\max}/\sigma_{\mathrm{Y}}\right)^2\right)^{3.225\,1}\right]^{0.759\,52} \end{cases}$$

(C)1994-2021 China Academic Journal Electronic Publishing House. All rights reserved. http://www.cnki.net

$$\Delta K_{\mathrm{effth}}(R)=\begin{cases}K_{\max}\left(a_{\mathrm{th}}\right)\cdot\left[1-f_{\mathrm{op}}\left(a_{\mathrm{th}}\right)\right], R<0.7\\ \Delta K_{\mathrm{th}}(R), \qquad\qquad R\geqslant 0.7\end{cases}$$

where A is a material- and environmentally-sensitive constant of dimensions $(\mathrm{MPa})^{-2}$; m is a constant representing the slope of the corresponding fatigue crack growth rate curve; n is the index indicating the unstable fracture; K_{Ic} is the plane strain fracture toughness of the material; K_{Cf} is the fracture toughness of the material under fatigue loading; r_{e} is an empirical material constant of the inherent flaw length of the order of 1 mm; a is the modified crack length which is equal to r_{e} plus the actual crack length; $\sigma_{\max}$ is the maximum applied stress; $\sigma_{\min}$ is the minimum applied stress; $Y(a)$ is a geometrical factor; $Y(r_{\mathrm{e}})$ is a geometrical factor when a is equal to r_{e}; R is the stress ratio $(=\sigma_{\min}/\sigma_{\max})$; ΔK_{th} is the threshold value of stress intensity factor range; a_{th} is the threshold value corresponding to ΔK_{th}; ΔK_{eff} is the effective range of the stress intensity factor; $\Delta K_{\mathrm{effth}}$ is the effective range of the stress intensity factor at the threshold level; K_{op} is the stress intensity factor at the opening level; α' is the crack tip stress/strain constraint ratio, which is 1 for the plane stress state and $1/(1-2\nu)$ for the plane strain state. The effect of n is significant only in the unstable propagation region; a constant value of 6 is recommended for a quick and simple engineering analysis. It is generally assumed that $K_{\mathrm{Cf}}=K_{\mathrm{IC}}$.

Fig.8 is the crack growth rate curve simulated by UCGRM. All the model parameters are listed with the curve. The model will be used for calculating the crack length in 3D simulation.

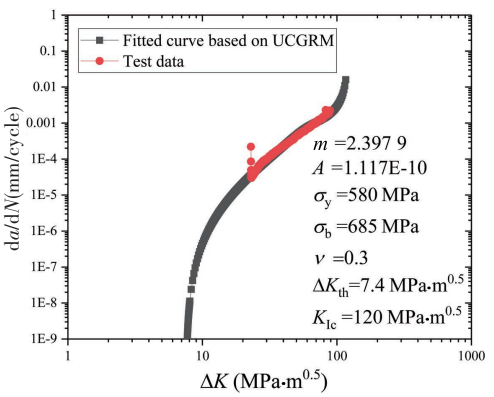

Fig.8 Crack growth rate curve simulated by UCGRM with model parameters

2 Theoretical and numerical analysis

2.1 Failure criteria

The failure form of a general internal pressure chamber includes leakage, rupture and excessive deformation or even destruction. Failure criteria can be divided into strength failure criteria and stiffness failure criteria. Strength failure criteria includes elastic failure, plastic failure, elastic-plastic failure, fatigue failure, fracture failure and corrosion failure etc. and stiffness failure criteria typically refer to those of leakage and structural loss stability. Sometimes, an acceptable critical dimension is artificially defined to limit the extent of defect expansion before ensuring that the structure does not break. The plasticity and toughness of this 20MnMoNb steel are very strong, especially the fracture toughness reaching more than 120 $\mathrm{MPa\cdot m^{0.5}}$. In the design stage, the deformation of the structure will be checked and the excessive deformation damage of the cylinder will not occur when the structure is used properly. In the stage of crack propagation, high fracture toughness prevents the occurrence of unstable propagation. Therefore, in the service life calculation based on fracture mechanics, the failure criterion proposed in this paper is the criterion of acceptable crack

(C)1994-2021 China Academic Journal Electronic Publishing House. All rights reserved. http://www.cnki.net

sizes.

2.2 Modelling approach

2.2.1 Simulation validation

A general finite element software Abaqus and a special analytical software for three-dimensional crack propagation Franc3D were combined to simulate the fatigue crack growth of structure for the present study. The accuracy of the stress intensity factors at the crack front determines the accuracy of the simulation results. Therefore, the calculation results of stress intensity factor at crack tip of standard CT specimens were compared with those from Franc3D software firstly.

Before the finite element calculation, the material properties of CT samples were defined according to the experimental results of 20MnMoNb as listed in Tab.1 and the Poisson's ratio was 0.3. The surfaces of the two cylindrical holes contacted with the pins were coupled to their respective centers and loaded with a concentrated force of 20 kN at the two points of the coupling. The loads were directed toward both sides of the specimen and the boundary conditions were applied on the central line of the surface farther away from the circular hole. Fig.9 shows the comparison between the a–N curves by test and simulation. The calculated results of stress intensity factor at crack tip of CT specimens obtained by Franc3D simulation were compared with those obtained by formula, as shown in Fig.10. According to the comparison of the curves in the figure, it can be seen that the calculated stress intensity factors of Franc3D software are in good agreement with those from the formula except for some deviated points from unstable calculation. Then the model can be used for numerical simulation of fatigue crack growth with satisfactory accuracy.

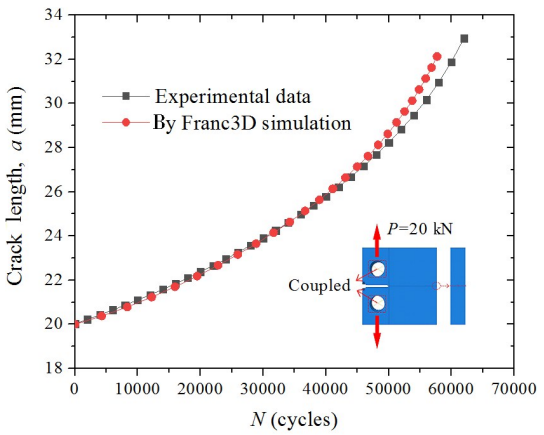

Fig.9 Comparison between the a–N curves by test and simulation

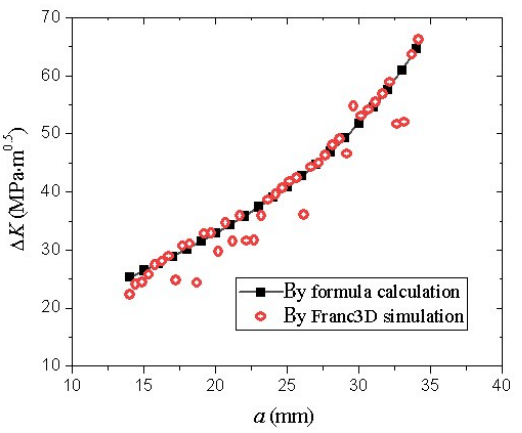

Fig.10 Comparison between the ΔK–a curves from test and simulation

2.2.2 3D simulation of surface cracks analysis

For a cylindrical internal pressure vessel, the stress on the inner wall of the vessel is the largest, and the internal defects of the material are most likely to occur there. It is assumed that a semi-elliptical macro-surface crack occurs on the inner wall of the chamber as shown in Fig.11 and the semi-elliptical crack is also a simplified form of the general surface cracks. The crack will be calculated through the sub-model of the cylindrical structure after mesh refinement in Franc3D software. a and c are respectively the short and long half-axis lengths of a semi-elliptical shape, i.e. crack depth and surface half-length. The initial size of the crack, c_0=5 mm and a_0=3 mm, is presumed for

(C)1994-2021 China Academic Journal Electronic Publishing House. All rights reserved. http://www.cnki.net

initial analysis. When the maximum value of the cyclic internal pressure is 110 MPa, the variation of crack dimensions with the number of loading cycles can be calculated, as shown in Fig.12. When the number of cycles is 150 000, the crack depth grows to 65 mm and the length reaches 95 mm. The thickness of the cylinder is 220 mm, that is to say, after 150 000 times, the assumed macroscopic crack depth has reached 30% of the thickness of the chamber.

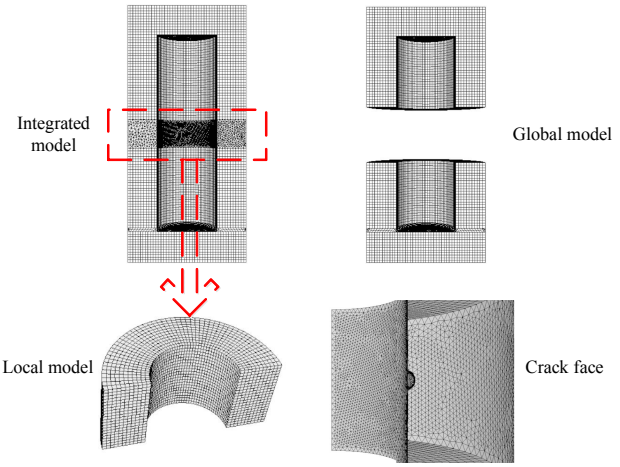

Fig.11 FE global model and sub-model with a surface crack

If one tenth of the wall thickness is taken as the acceptable crack depth, the loading cycles are about 110 000 times. The ultimate strength test frequency by using the present pressure cylinder is about 400 times per year, or about 12 000 times in 30 years. If we consider cyclic loading tests of some special components, the frequency of loading cycles can be increased by 200 times a year according to the current frequency records, then it is about 18 000 cycles in thirty years. Under the current criterion that the crack depth is less than one tenth of the wall thickness, the life requirement is satisfied. And according to the analysis, the service life of the pressure cylinder in the design pressure state is about six times the safety margin.

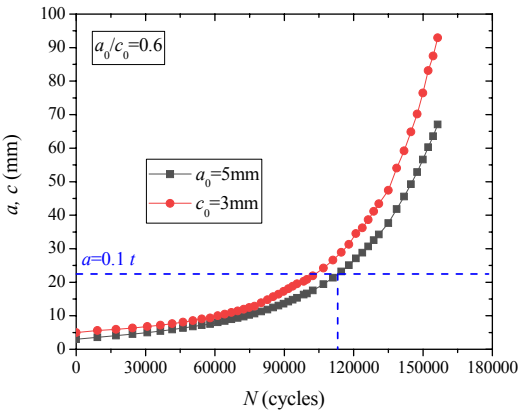

Fig.12 Crack length versus cycles when c_0= 5 mm and a_0=3 mm respectively

2.2.3 Effect of initial aspect ratio and crack inclination on crack growth properties

Crack characteristics are one of the factors affecting life. The influences of aspect ratio of an

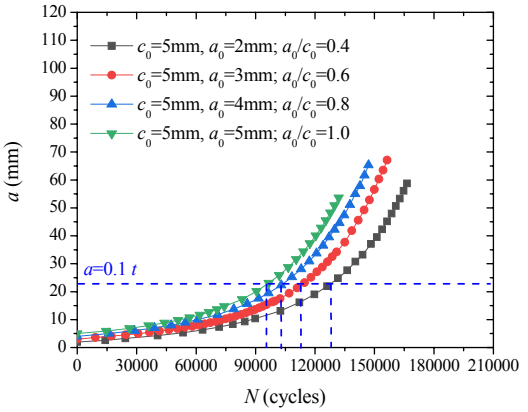

Fig.13 Effects of initial aspect ratio on crack growth in depth direction when c_0 is set to 5 mm

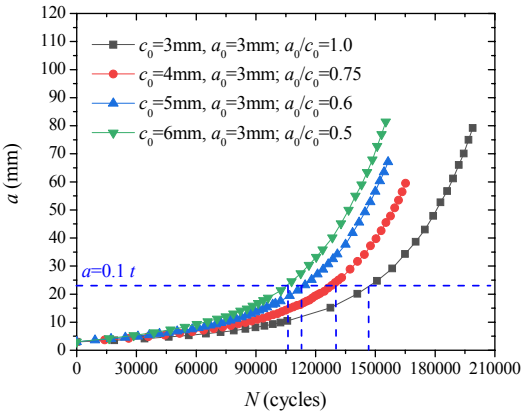

Fig.14 Effects of initial aspect ratio on crack growth in length direction when a_0 is set to 3 mm

(C)1994-2021 China Academic Journal Electronic Publishing House. All rights reserved. http://www.cnki.net

initial crack and angle of crack relative to the center axis of the pressure cylinder on life will be analyzed in this section. The acceptable crack size is still 1/10 of the cylinder wall thickness. Figs.13–14 show the crack growth curves under different initial aspect ratios. Fig.10 presents the analysis of the crack growth at different initial depths under the same initial crack half-length c_0 of 5 mm while Fig.13 shows the crack growth with different initial lengths at the same initial crack depth a_0 of 3 mm. When the initial crack length was 5 mm, the crack growth at initial depths of 2 mm, 3 mm, 4 mm and 5 mm was investigated. The minimum residual life was 96 668 cycles. When the initial crack depth was fixed to 3 mm, the crack growth was investigated when the initial length was 3 mm,

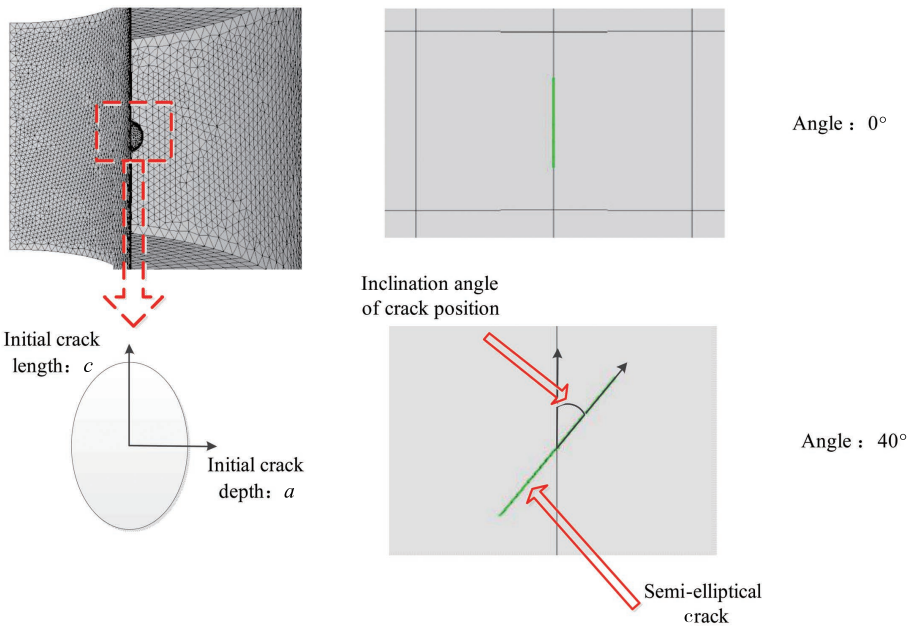

Fig.15 Configuration of surface crack inclination in FE model

4 mm, 5 mm and 6 mm respectively. The minimum residual life was 102 566 cycles. The remaining life can meet the application requirement.

The effect of the crack inclination angle to the cylinder axis was also studied under the condition of a_0=3 mm and c_0=5 mm. The configuration of the surface crack inclination in the FE model is shown in Fig.15. The inclination angles of cracks are 0°, 5°, 10°, 20° and 30° respectively. Results in Fig.16 show that the angle of inclination retards crack growth. Then conservative calculation can be done by not taking inclination into account.

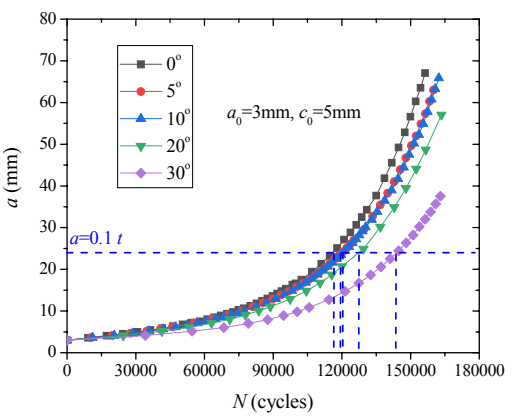

Fig.16 Effects of inclination on crack growth in depth direction when a_0=3 mm and c_0=5 mm

3 Conclusions

UHP chambers used to simulate deep-sea environment need to bear a pressure of more than

(C)1994-2021 China Academic Journal Electronic Publishing House. All rights reserved. http://www.cnki.net

110 MPa. After several years of use, the UHP chambers need to be checked in a comprehensive way. The residual life of a certain aged UHP chamber under the condition of cracking was studied. One tenth of the chamber's wall thickness was defined as the allowable depth of surface cracks on the inner wall. Based on this criterion, the residual life of the chamber was analyzed under the assumption that there were macroscopic inner surface cracks.

The UHP chambers sometimes withstand trapezoidal load with holding time at peak stress in service. Therefore, in this paper, the sensitivity of material to topographic load was studied experimentally at first. The sustaining time of 2 min at peak stress was set for each cycle. The experimental results were compared with those under triangular fatigue load, which proves that the material is not sensitive to holding time. The material parameters obtained from conventional fatigue crack growth test can be used to evaluate the crack growth in UHP chambers.

Franc3D was used to calculate the crack growth, and its accuracy was verified by comparing the computed results of CT test with the experimental results. The crack growth with different initial sizes and depth to length ratios is analyzed, and the effect of the crack inclination angle to the cylinder axis was studied. Results show that the angle of inclination retards crack growth, and that, under the current criterion, the crack depth is less than one tenth of the wall thickness, and the life requirement is satisfied. According to the analysis, the service life of the pressure cylinder in the design pressure state is about six times the safety margin. The analysis results can be used as a reference for evaluation of the reliability of UHP chambers.

References

[1] Cui W C, Huang X P, Wang F. Towards a unified fatigue life prediction method for marine structures[M]. Springer, 2014.

[2] Li T. Research on the deep-sea pressure environmental simulation test device and its constant pressure control system[D]. Harbin: Harbin Engineering University, 2013

[3] Liang Z, Zhao Y, Jiang F G. Design and strength analysis of high pressure simulation test vessel[J]. China Petroleum Machinery, 2015, 43(7): 61-74.

[4] Jiang F G, Li Z L, Liang Z, et al. Design and analysis of the sealing device for high pressure/large diameter simulating deep water cabins[J]. China Offshore Oil and Gas, 2016, 28(6): 121-127.

[5] Huang H C, Shen Y, Yang Z G, et al. A deep-sea large-volume high-pressure simulation system-Design, analysis and experimental verification[J]. Ocean Engineering, 2019, 180: 29-39.

[6] Wang F, Zhang S J, Yu S, et al. Design and analysis on a model sphere made of maraging steel to verify the applicability of the current design code[J]. Ships and Offshore Structures, 2019, 14(1): 86-94.

[7] Wang F, Wang K, Cui W C. A simplified life estimation method for the spherical hull of deep manned submersibles[J]. Marine Structures, 2015, 44: 159-170.

[8] Zhang J, Zhang M, Cui W C, et al. Elastic-plastic buckling of deep sea spherical pressure hulls[J]. Marine Structures, 2018, 57: 38-51.

[9] Sun F L, Ren S, Li Z, et al. Comparative study on the stress corrosion cracking of X70 pipeline steel in simulated shallow and deep sea environments[J]. Materials Science and Engineering: A, 2017, 685: 145-153.

[10] Yang Z X, Kan B, Li J X, et al. Hydrostatic pressure effects on corrosion behavior of X70 pipeline steel in a simulated deep-sea environment[J]. Journal of Electroanalytical Chemistry, 2018, 822: 123-133.

[11] Margolin B Z, Karzov G P. Fatigue failure of nuclear pressure vessel steels-II. Prediction of fatigue crack propagation[J]. International Journal of Pressure Vessels and Piping, 1997, 74(2): 111-120.

(C)1994-2021 China Academic Journal Electronic Publishing House. All rights reserved. http://www.cnki.net

[12] Price J W H, Ibrahim R N. Crack growth in aluminium cylinders[J]. International Journal of Pressure Vessels and Piping, 2000, 77(13): 831-836.

[13] Tan X M, Wang G Z, Tu S T, et al. Creep constraint and fracture parameter C^* for axial semi-elliptical surface cracks with high aspect ratio in pressurized pipes[J]. Engineering Fracture Mechanics, 2018, 199: 358-371.

[14] Pennell W E, Corwin W R. Reactor pressure vessel structural integrity research[J]. Nuclear Engineering and Design, 1995, 157(1-2): 159-175.

[15] Zhang W, Zhang S K, Cui W C, et al. Stress intensity factor research about a thick-walled cylinder with an internal semi-elliptical surface crack[J]. Journal of Ship Mechanics, 1999, 3(4): 49-53.

[16] Shlyannikov V N. Fatigue shape analysis for internal surface flaw in a pressurized hollow cylinder[J]. International Journal of Pressure Vessels and Piping, 2000, 77(5): 227-234.

[17] Shariati M, Mohammadi E, Nejad R M. Effect of a new specimen size on fatigue crack growth behavior in thick-walled pressure vessels[J]. International Journal of Pressure Vessels and Piping, 2017, 150: 1-10.

[18] Wang F, Cui W C. Experimental investigation on dwell-fatigue property of Ti-6Al-4V ELI used in deep-sea manned cabin [J]. Materials Science and Engineering: A, 2015, 642: 136-141.

[19] Wang F, Jiang Z, Cui W C. Low-cycle dwell-fatigue life and failure mode of a candidate titanium alloy material TB19 for full-ocean-depth manned cabin[J]. Journal of Ship Mechanics, 2018, 22(6), 727-735.

深海超高压环境模拟容器裂纹评定

吴 冕[1], 王 芳[2,3], 罗瑞龙[3], 姜 哲[3], 崔维成[3,4]

(1. 江苏科技大学 江苏省船海机械先进制造及工艺重点实验室, 江苏 镇江 212003;
2. 上海海洋大学 工程学院, 上海海洋可再生能源工程技术研究中心, 上海 201306;
3. 上海海洋大学 海洋科学学院, 上海深渊科学工程技术研究中心, 上海 201306;
4. 西湖大学 工学院, 杭州 310024)

摘要: 深海超高压环境模拟容器用于模拟水下压力环境,其容器壁上承受反复载荷,容易产生疲劳裂纹。疲劳裂纹扩展是影响其断裂的主要因素。本文旨在分析半椭圆裂纹在老化的深海超高压环境模拟容器中的扩展行为,评估容器的安全性,因此对材料20MnMoNb钢的裂纹扩展特性进行了试验研究,首先考虑三角形和梯形加载情况,通过比较两组实验结果,考察了其材料对保载时间的敏感性。采用基于统一的裂纹扩展率模型的三维有限元方法进行了疲劳裂纹扩展计算,并通过CT试样的一组数值和实验结果进行了验证,最后建立了不同初始尺寸、展弦比和倾角的裂纹有限元模型,并根据裂纹在容器内壁的容许深度准则,计算了容器的剩余寿命。其分析结果可为深海超高压环境模拟容器可靠性评估提供参考。

关键词: 超高压舱; 裂纹扩展; 压力容器; 深海环境模拟; 剩余寿命

中图分类号: U663.8 **文献标识码:** A

基金项目: 国家自然科学基金资助项目(52071203);上海市科委自然科学基金一般项目(19ZR1422700);
上海海洋可再生能源工程技术研究中心项目(19DZ2254800)

作者简介: 吴 冕(1993-),男,江苏科技大学硕士研究生;
王 芳(1979-),女,博士,上海海洋大学副研究员;
罗瑞龙(1986-),男,博士,上海海洋大学讲师;
姜 哲(1982-),男,博士,上海海洋大学研究员;
崔维成(1963-),男,博士,西湖大学/上海海洋大学教授。

(C)1994-2021 China Academic Journal Electronic Publishing House. All rights reserved. http://www.cnki.net